

NUMERICALLY MODELING MERCURIAN IMPACTS: THE FORMATION OF CALORIS BASIN AND THE ORIGIN OF ITS LOW-REFLECTANCE MATERIAL.

Ross, W. K. Potter^{1,2} and James W. Head^{1,2},
¹Department of Earth, Environmental and Planetary Sciences, Brown University, Providence, RI, 02912, USA,
²NASA Solar System Exploration Research Virtual Institute, ross_pottter@brown.edu.

Introduction: Mariner 10 [1] and MErcury Sur- face, Space ENvironment, GEochemistry and Ranging (MESSENGER) [2] imagery revealed the presence of a ~1500 km diameter [3,4] impact basin on Mercury - Caloris. Located in Mercury's north east quadrant, the basin is the largest observed mercurian impact structure and thought to have formed ~3.9 Ga [5]. The basin is infilled by what has been interpreted as smooth volcanic deposits [3], like much of Mercury's northern latitudes [3,6], complicating interpretations of the basin's original structure. Additional tectonic deformation has also occurred; parts of Caloris' interior now exceed its rim height by ~1 km [7]. The smooth volcanic deposits within the basin have a 20% higher reflectance than the global mean and are referred to as High-Reflectance Red Plains (HRP) material. A second unit – Low-Reflectance Material (LRM) - is also present within Caloris and so-called as its reflectance is 15% lower than the global mean. The LRM is exposed within craters and ejecta, suggesting it resides beneath the HRP. [8,9] estimate the LRM to be a minimum of 7.5-8.5 km thick and possibly representative of the original basin floor material. LRM may, therefore, have a lower crustal and/or upper mantle composition [9].

In this work, numerical modeling of Caloris-sized basin-forming impacts is conducted to investigate the formation of Caloris and the origin of its LRM. Concurrently, this provides insight into general basin formation on Mercury, which may differ to that on the Moon [10] and possibly be a result of Mercury's substantial core.

Methods: The iSALE shock physics code [e.g., 11] was used to numerically model Caloris-sized basin-forming events. Impacts were simulated into both half-space and fully spherical targets divided into a basalt [12] crust, dunite [13] mantle and iron [14] core. The silicate (crust and mantle) portion of the target was 400 km thick [15], which included a 50 km thick crust [16]. Two thermal profiles, based on previous work [17], were used. These had crustal and upper mantle thermal gradients of 8 and 15 K/km. As with previous modeling of large-scale basin-forming events [18], a partial melt viscosity, providing super solidus material some resistance to shear, and acoustic fluidization, to help facilitate crater collapse, were included. Impactor diameter and velocity ranges were 50-250 km and 15-50 km/s, respectively. Cell size was 5 km. For the half-space models, surface gravity was a constant 3.7 m/s².

For the spherical target models, the gravity field above Mercury's surface decayed in magnitude with radial distance squared.

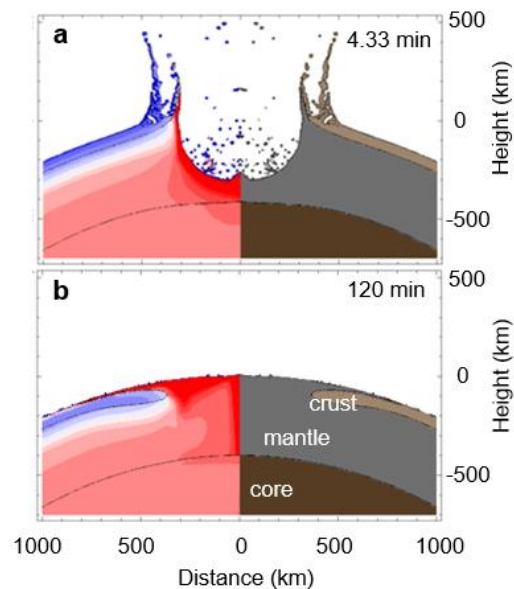


Figure 1: Transient (a) and final (b) crater for a Caloris-sized impact (100 km diameter impactor; 42 km/s velocity; 8 K/km thermal gradient). Left panels show temperature (blue is low, red is high); right panels show material (crust, beige; mantle, gray; core, brown).

Results: Figure 1 illustrates the transient (a) and final (b) craters for a Caloris-sized impact (100 km diameter impactor, 42 km/s velocity) into the 8 K/km thermal gradient target. Final basin size was constrained by the continuous surficial extent of mantle (an analogy for the extent of basin floor material). Mantle material extends to radial distances of ~800 km from the basin center. This material is partially or completely molten. Total mantle melt volume was $9 \times 10^7 \text{ km}^3$, which exceeds the transient crater volume ($\sim 7 \times 10^7 \text{ km}^3$). Note in Figure 1a, that the transient crater does not penetrate into Mercury's core. Figure 2 demonstrates that for Caloris, and smaller basin-forming impacts, maximum excavation depth and transient crater depth are within the mantle. For the impact shown in Figure 1, the transient crater and excavation depth were 340 km and 82 km, respectively.

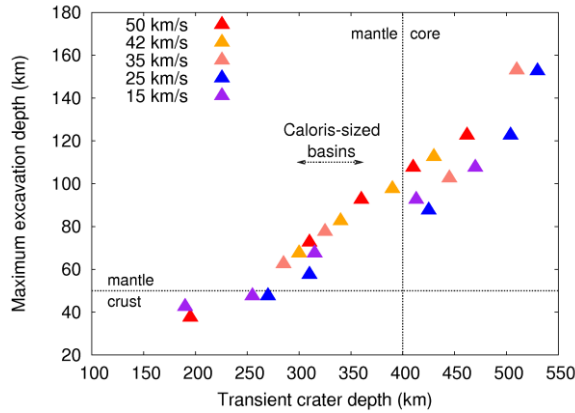


Figure 2: Excavation depth as a function of transient crater depth for a suite of mercurian basin-forming impacts. Caloris-sized basins will excavate mantle but their transient craters will not penetrate into the core.

Discussion:

Impact melt and the LRM. The Caloris impact may have partially melted material to a depth of 220 km and formed a melt sheet 3-15 km thick [9] which could equate to the thickness of the LRM. Total mantle melt volumes in the models were on the order of 10^7 km^3 , greater than that predicted for Mercury's volcanic northern smooth plains ($10^6\text{-}10^7 \text{ km}^3$ [19]). A volume of melt of this magnitude should undergo differentiation [20] forming a lower density crustal-like layer towards the surface. Gravity suggests a 20 km thick crust beneath Caloris [16]. Differentiation of impact melt could, therefore, explain the discrepancy between the models (no crust at the basin center) and the gravity data.

The models, therefore, suggest that Caloris LRM could be differentiated molten mantle material. LRM-like, low albedo deposits have also been recognized around other large mercurian basins (e.g., Rembrandt) and interpreted as impact melt [21]. These complement [22] who suggested the darkening agent responsible for the LRM is an intrinsic component of Mercury's crust and/or mantle. A source depth of 30 km has been estimated [23], which further implies lower crust and, possibly, mantle.

Basin formation. The models suggest basin formation on Mercury is comparable to that on the Moon (e.g., [18]). Pi-scaling relationships (e.g., [24]) demonstrate that mercurian basin-forming impacts follow the same trends as lunar basins (e.g., Figure 3). The models also demonstrate that Mercury's core does not affect Caloris-sized basins, and, by extension, smaller-sized basins. Core interaction may play a role for basins larger than Caloris, though there is no evidence on Mercury for these larger basins [10]. Differences in

size and number of basins between Mercury and the Moon is, therefore, most likely due to longer term factors such as basin relaxation, and volcanic and tectonic modification.

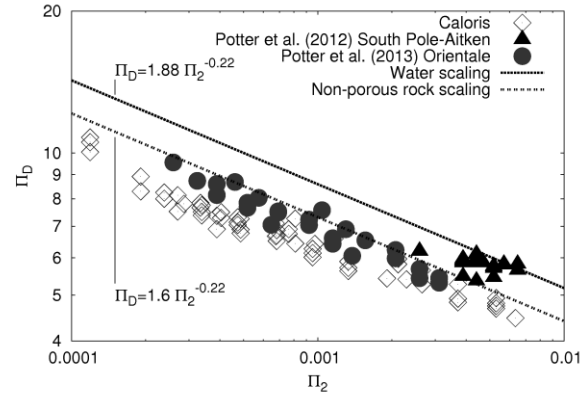


Figure 3. Π_D as a function of Π_2 . Π_D is a crater size measure defined as $D_{ic}/(M_i/\rho_i)^{1/3}$. Π_2 is a gravity-scaled impact size defined as $3.22 g r_i/u^2$. D_{ic} : transient crater diameter; M_i : impactor mass; ρ_i : target density; g : surface gravity; r_i : impactor radius; u : impact velocity. Scaling laws from [24].

References: [1] Murray, B. C. et al. (1974) *Science*, 185, 169-179. [2] Solomon, S. C. et al. (2008) *Science*, 321, 59-62. [3] Murchie, S. L. et al. (2008) *Science*, 321, 73-76. [4] Fassett, C. I. et al. (2009) *EPSL*, 285, 297-308. [5] Marchi, S. et al. (2013) *Nature*, 499, 59-61. [6] Head, J. W. et al. (2011) *Science*, 333, 1853-1856. [7] Oberst, J. F. et al. (2010) *Icarus*, 209, 230-238. [8] Ernst, C. M. et al. (2010) *Icarus*, 209, 210-223. [9] Ernst, C. M. et al. (2015) *Icarus*, 250, 413-429. [10] Fassett, C. I. et al. (2012) *JGR*, 117, E00L08. [11] Collins, G. S. et al. (2004) *MAPS*, 39, 217-231. [12] Pierazzo, E. et al. (2005) *GSA Spec. Pap.* 384, 443-457. [13] Benz, W. et al. (1989) *Icarus*, 81, 113-131. [14] Thompson, S. L. and Lauson, H. S. (1972) Sandia National Laboratory Report SC-RR-71 0714. [15] Hauck, S. A. et al. (2013) *JGR Planets*, 118, 1204-1220. [16] Smith, D. E. et al. (2012) *Science*, 336, 214-217. [17] Zuber, M. T. et al. (2010) *Icarus*, 209, 247-255. [18] Potter, R. W. K. et al. (2013) *JGR Planets*, 118, 963-979. [19] Ostrach, L. R. et al. (2015) *Icarus*, 250, 602-622. [20] Vaughan, W. M. et al. (2013) *Icarus*, 223, 744-765. [21] Whitten J. L. and Head, J. W. (2015) *Icarus*, 258, 350-365. [22] Murchie, S. L. et al. (2015) *Icarus*, 254, 287-305. [23] Rivera-Valentin, E. G. and Barr, A. C. (2014) *EPSL*, 391, 234-242. [24] Schmidt, R. M. and Housen, K. R. (1987) *Int. J. Imp. Eng.*, 5, 543-560.